IC/82/59
INTERNAL REPORT
(Limited distribution)

International Atomic Energy Agency
and
United Nations Educational Scientific and Cultural Organization

INTERNATIONAL CENTRE FOR THEORETICAL PHYSICS

HIGH TEMPERATURE INTERNAL FRICTION IN PURE ALUMINIUM*

J.K. Aboagye**
International Centre for Theoretical Physics, Trieste, Italy,

and

D.S. Payida
Department of Physics, University of Cape Coast,
Cape Coast, Ghana.

MIRAMARE - TRIESTE
May 1982

* To be submitted for publication.

** On leave of absence from Department of Physics, University of Cape Coast, Cape Coast, Ghana.

ABSTRACT

The temperature dependence of internal friction of nearly pure aluminium (99.99% aluminium) has been carefully measured as a function of annealing temperature and hence grain size. The results indicate that, provided the frequency and annealing temperature are held constant, the internal friction increases with temperature until some maximum value is attained and then begins to go down as the temperature is further increased. It is also noted that the internal friction decreases with annealing temperature and that annealing time has the same effect as annealing temperature. It is also noted that the internal friction peak is shifted towards higher temperatures as annealing temperature is increased. It is surmised that the grain size or the total grain boundary volume determines the height of the internal friction curve and that the order-disorder transitions at the grain boundaries induced by both entropy and energy gradients give rise to internal friction peaks in polycrystals.

INTRODUCTION

The property which gives rise to the attenuation or damping of lattice vibrations of solids by the transformation of mechanical energy into thermal energy is known in metallurgy as internal friction. According to the classical theory of elasticity based on Hooke's law, stress waves are transmitted by a perfectly elastic solid with the following characteristics:

(a) The strain at any point in the body is a function only of the instantaneous stress at the point;

(b) On removal of the stress the elastic strain is instantaneously and fully recoverable;

(c) Since the classical process of elastic deformation is reversible, there is no dissipation of energy. Such a process can only occur if the deformation is performed quasi-statically, that is equilibrium is established in the body at every instant of time. Thus a travelling pulse or sine wave would then have constant energy and an isolated perfectly elastic solid, when set into vibration, would continue to vibrate indefinitely.

Experimental measurements on real solids reveal the presence of energy dissipation even at very small strains. This dissipation of energy is associated with non-elastic behaviour of the body.

We may examine the phenomenon of internal friction by reference to Zener's equation i.e.

$$\sigma + \tau_1 \dot{\sigma} = M_R (\epsilon + \tau_2 \dot{\epsilon}) , \qquad (1)$$

where τ_1 = relaxation time of the stress under constant strain,
τ_2 = relaxation time of the strain under constant stress,
M_R = ratio of stress to strain after the system has completely relaxed = the relaxed elastic modulus,
σ = stress,
ϵ = strain,

1) For a constant stress σ_o applied suddendly at t=0, equation (1) has the solution

$$\epsilon(t) = \frac{\sigma_o}{M_R} + \left(\epsilon_o - \frac{\sigma_o}{M_R} \right) \exp\left(- \frac{t}{\tau_2} \right) , \qquad (2)$$

where ϵ_o is the Hookean strain at time t=0.

This behaviour of real materials is depicted in fig. 1 below

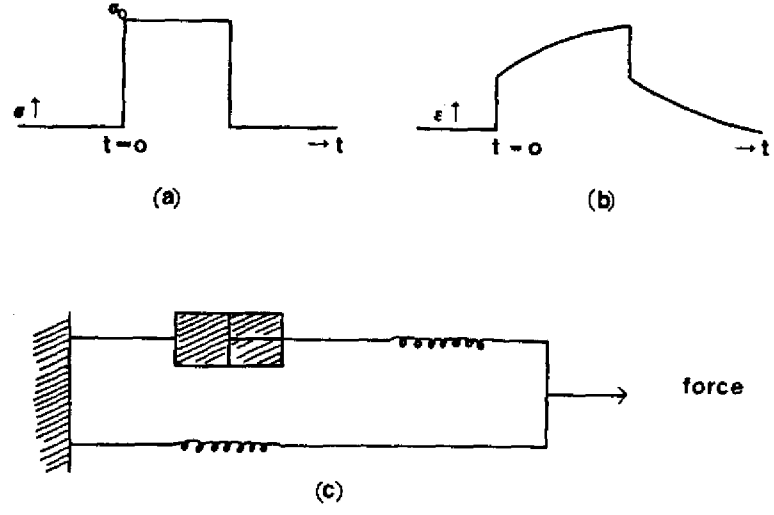

Fig. 1

(a) applied stress pulse

(b) resulting strain

(c) equivalent mechanical model (has the same form of equation of motion).

2) For a constant strain ϵ_o suddendly applied at t=0 the solution of equation (1) is

$$\sigma(t) = M_R \epsilon_o + \left(\sigma_o - M_R \epsilon_o \right) \exp\left(- \frac{t}{\tau} \right) , \qquad (3)$$

i.e. there is an instantaneous σ_o followed by a gradual decrease to the value $M_R \epsilon_o$ as shown in fig. 2

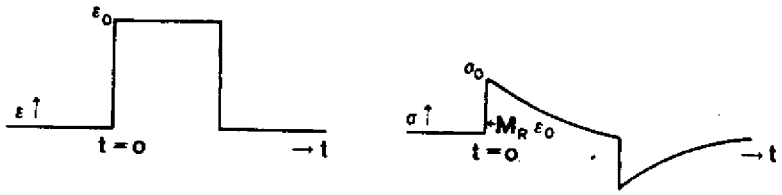

Fig. 2

Stress-time relationship at constant strain for a Zener solid.

Energy dissipation or internal friction

The viscuous elements in the theoretical models described give rise to energy dissipation or internal friction. If stress and strain are periodic functions of time, we may write

$$\left.\begin{aligned}\sigma &= \sigma_0 \exp(i\omega t)\\ \epsilon &= \epsilon_0 \exp[i(\omega t - \delta)]\end{aligned}\right\}, \tag{4}$$

where in general there will be a phase difference, δ, between stress and strain. Substitution of equations (4) in equation (1) gives

$$(1+i\omega\tau_1)\sigma = M(1+i\omega\tau_2)\epsilon \ . \tag{5}$$

We may write this expression as

$$\sigma = M^*\epsilon \ , \tag{6}$$

where

$$M^* = \frac{1+i\omega\tau_2}{1+i\omega\tau_1} M_R \tag{7}$$

and is called the complex modulus.

In this case the phase angle δ will be given by

$$\tan\delta = \frac{\mathrm{Im}\, M^*}{\mathrm{Re}\, M^*} = \frac{\omega(\tau_2-\tau_1)}{1+\omega^2\tau^2} \ , \tag{8}$$

where

$$\tau = (\tau_1\tau_2)^{1/2} \ . \tag{9}$$

We may also define a mean modulus $\bar{M}$ such that

$$\bar{M} = (M_U M_R)^{1/2} \ . \tag{10}$$

where

$$M_U = \frac{\tau_2}{\tau_1} M_R = \frac{\Delta\sigma}{\Delta\epsilon} \ , \tag{11}$$

i.e. M_U is the unrelaxed elastic modulus.

Equation (8) may then be written with the aid of equation (11) to give

$$\tan\delta = \frac{M_U - M_R}{\bar{M}} \frac{\omega\tau}{1+(\omega\tau)^2} \ . \tag{12}$$

This form of the equation for tan δ has the same form as the Debye relaxation equation in the theory of dielectric relaxation. Hence tan δ is a convenient measure for the energy loss in analogy with the corresponding quantity used in electric circuit theory.

We can write the energy dissipated per cycle, ΔE as

$$\Delta E = \int_0^{2\pi/\omega} \sigma\dot{\epsilon}\, dt = \pi\sigma_0\epsilon_0 \sin\delta \ . \tag{13}$$

The energy loss is often expressed in terms of the loss factor, Q^{-1} where

$$Q^{-1} = \frac{1}{2\pi}\frac{\Delta E}{E} = \sin\delta \approx \tan\delta \qquad (14)$$

if δ is small. The logarithmic decrement, Δ, may then be found from

$$\Delta = \pi Q^{-1} ,$$

i.e.

$$Q^{-1} = \frac{\Delta}{\pi} = \frac{1}{\pi}\ln\left[\frac{A(n)}{A(n+1)}\right], \qquad (15)$$

where A(n) is the n^{th} amplitude

and A(n+1) is the $(n+1)^{th}$ amplitude.

Thus a measurement of successive amplitudes gives a measure of the internal friction.

The relaxation time, τ, depends on time according to the equation

$$\tau = \tau_0 \exp\left(\frac{U}{kT}\right) , \qquad (16)$$

where U is an activation energy. Thus from equations (12) and (14) we conclude that the internal friction is a function of temperature T.

Effect of grain size

A polycrystalline material consists of an assembly of small single crystals (grains) oriented more or less at random. When a wave propagates through such a material the varying orientations of the grains result in some grains becoming more compressed than others with a consequent heat flow between grains. Zener (C. Zener, Elasticity and Anelasticity of Metals, University

of Chicago Press, Chicago, 1948) shows that the loss factor, η, due to this effect, is given by

$$\eta = Q^{-1} = \frac{C_p - C_v}{C_v} R \frac{\nu\nu_0}{\nu^2 + \nu_0^2} , \qquad (17)$$

where R is the fraction of the total strain energy associated with dilational changes, and ν_0 is the intergrain relaxation frequency

$$\nu_0 = \frac{D}{L_c^2} = \frac{K}{\rho C_p L_c^2} , \qquad (18)$$

where L_c is the mean diameter of the grains, D the thermal diffusivity, ρ the volume density and K the thermal conductivity.

The concept of viscuous grain boundary predicts that a change in grain size of the specimen will have the same effect as a change in the frequency of vibration. This is due to the fact that the relaxation time associated with the stress relaxation across grain boundaries increase with the increase of grain size. The total grain boundary volume is normally assumed as some simple function of grain size, i.e.

$$d \propto \frac{1}{V} , \qquad (19)$$

where d is the mean grain diameter and V the total boundary volume. Thus a study of d implies V and vice versa.

If applied stresses are small so there is no plastic deformation then Hooke's relation can be applied to the grain boundary i.e.

$$\sigma = \mu_{SB}\frac{X}{a} , \qquad (20)$$

where

σ = resolved shear stress,

μ_{SB} = boundary shear modulus,

x = mean displacement of atoms from equilibrium position,

a = mean equilibrium inter-atomic distance.

Since x is the mean atomic displacement from equilibrium position, it is directly proportional to the amplitude of oscillation due to an applied shear stress and therefore gives a measure of the amplitude of oscillation.

Equation (20) can be written as

$$X = \frac{\sigma a}{\mu_{SB}} \quad . \tag{21}$$

From this equation we find that a large boundary shear modulus μ_{SB} implies small amplitudes x and hence large internal friction and small μ_{SB} implies large amplitudes and hence low internal friction. It can be shown that x also varies as d^3 i.e.

$$X = k_2 d^3 \quad , \tag{22}$$

where k_2 = a constant and d = the mean grain diameter.

EXPERIMENTAL PROCEDURE AND RESULTS

In the study of the effect of grain size the specimens used were 99.99%, 99.999% and 99.5% aluminium wires with different diameters and lengths kindly provided by Goodfellow Metals of Science Park, Milton Road, Cambridge CB4, England. The stock materials consisted of aluminium wires of diameters 0.0005m and 0.0025m.

To anneal a wire sample, 0.30m of the wire was placed inside a test tube and the tube was closed by a cork cover. The tube was then heated in a Griffin Electric Furnace which was used for this purpose. To prevent oxidation the test tube was filled with the inert gas nitrogen. The wires were then annealed in turn at 200°C for 2 hours to remove all residual stresses and then

cooled down slowly in air at room temperatures. They were then annealed at temperatures of 250°C, 300°C, 400°C, 500° and 600°C for various time lapses in order to vary the grain size.

After annealing the wires were mounted in turn in a Ke's torsional pendulum (with some modification to suit local resources) and measurement of internal friction made from room temperature up to about 400°C, and then down again to room temperature. The internal friction was calculated from the decreases in the successive amplitudes (see equation (15)). The temperature was measured by using a Chromel-Alumel thermocouple which had been pre-calibrated at the boiling points.

RESULTS

From the observed set of successive amplitudes, the logarithmic decrement was determined for a number of successive pairs of amplitudes and an average logarithmic decrement computed and used in calculating the internal friction value for the corresponding temperature using the relation:

$$Q^{-1} = \frac{1}{\pi} \ln \left[\frac{A(n)}{A(n+1)} \right] .$$

In this way, sets of internal friction values with their corresponding temperatures were obtained. Tables (1 - 10) give these readings and these are displayed graphically in figures 3 and 4. Figure 5 gives the graph of the peak height of the internal friction as a function of annealing temperature for wires of the same diameter (0.00025m) and the same purity (99.99%). One finds that the peaks decrease with annealing temperature in agreement with equation (22).

Purity

A comparison of three different degrees of purity but same diameter and heat treatment shows an increasing tendency in the peaks with increasing

purity as shown in table 1 below.

% Purity	Diameter	Peak height (250°C)
99.5	0.500mm	0.086
99.99	0.500mm	0.093
99.999	0.500mm	0.105

Table 1

CONCLUSION

From the plots of internal friction values against temperature, some important features can be observed:

(a) For all the curves (figs. 3 and 4) the internal friction increases with temperature until it reaches a peak and then begins to decrease with increasing temperature;

(b) For the same wire annealed at a given temperature the internal friction decreases with annealing time (fig. 3) and the peak is shifted towards the high temperature and as the annealing time is increased;

(c) For the same wire annealed for a given time, the internal friction decreases with annealing temperature (figs. 4 and 5) and the peak is shifted towards the high temperature and as the annealing temperature is increased.

Figure 5 shows that the internal friction peak decreases with increasing temperature of annealing, in agreement with equation (22). From equation (22) we infer that a small d, the mean grain diameter, implies a small amplitude (high damping) and therefore high internal friction. A sample annealed at a higher temperature would have larger grains than a sample annealed at a lower temperature for the same length of time, and again from equation (22) a larger grain diameter would give rise to a smaller peak. The non-linear nature of the

plot shows that the peak is not a simple linear function of annealing temperature, hence there could be other factors that are contributory to the internal friction.

From Table 1 we find that the peak height increases with increasing purity. This is because impurities in a polycrystal are usually found in the grain boundaries and any annealing of the polycrystal drives impurity atoms from the crystal into the grain boundaries to further increase the impurity concentration at the grain boundary. This has the net effect of decreasing the grain boundary volume, and thus the internal friction in the less pure sample is smaller as compared to the pure one.

The general shape of internal friction curve does not change with annealing temperature or annealing time though the peak height changes; but the general trend remains the same. And since annealing fixes the grain size we conclude that the occurrence of the peak in the internal friction cannot be attributed to the mean grain diameter though the peak height is affected by the grain diameter. From equation (22) we find that a set of wires with the same purity but different grain diameters would have different internal friction. Thus the magnitude of the mean grain diameter should affect only the height of the peak; and the peaks should increase in height with decreasing grain boundary volume (see fig. 5). This mechanics model leads to two conclusions:

(i) the order-disorder transitions at the grain boundaries induced by both entropy and energy gradients give rise to internal friction peaks in polycrystals;

(ii) the total grain boundary volume determines the peak value of the internal friction.

ACKNOWLEDGEMENT

One of the authors (J.K.A.) would like to thank Professor Abdus Salam, the International Atomic Energy Agency and UNESCO for hospitality at the International Centre for Theoretical Physics, Trieste.

M.S. Amad, D.A. Barrow, E.A. Litte and Z.C. Szkopiak, J. Appl. Phys., 4, 1460 (1971).

E.A. Attia, J. Appl. Phys., (J. Phy. D.) G.B. Seriel 2, 1, No. 11, 1431 (1968).

G.S. Baker and S.H. Carpenter, Review of Science Instruments (U.S.A.), 36, No. 1, 29 (1965).

L.F. Balamuth, Phys. Rev., 45, 715 (1934).

A. Barnes and C. Zener, Phys. Rev., 58, 872 (1940).

K. Bennewitz and H. Rotger, Physics Zeits, 37, 578 (1936).

T.S. Ke, Phys. Rev., 71, 533 (1947).

T.S. Ke, Phys. Rev. LXX III, 267L (1948).

T.S. Ke, Phys. Rev. 72, 41 (1947).

J.S. Koehler, Impenfections in Nearly Perfect Crystals, (John Willey ans Sons, N.Y., 1952).

I. Kunihiko, M. Koiwa and R.R. Hasiguti, J. Phys. Soc. Jap., 39, No. 1, 117 (1975).

G.M. Leak, Proc. Phys. Soc., 78, 1528 (1961).

W.P. Mason, Fundamental Aspects of Dislocation Theory, (Academic Press, 1966).

C. Kittel, Introduction to Solid State Physics, (5th edition), (John Willey and Sons, 1976).

S.L. Quimby, Phys. Rev., 39, 345 (1932).

R.H. Randal, F.C. Rose and C. Zener, Phys. Rev., 56, 343 (1939).

H.F. Pollard, Sound Waves in Solids, (Pion Limited, London, 1977).

I.T. Suprun, J. Sov. Phys., 1, 72-75 (1976).

Numerical Internal Friction Data for 99.999%

Al Wire Diameter 0.0005m

Annealed at 250°C for 4 Hours

Temperature °C	Internal Friction (Q^{-1})
25.0	0.002
45.0	0.004
62.51	0.006
90.03	0.015
100.20	0.016
138.41	0.041
148.0	0.062
182.0	0.104
225.0	0.128
255.0	0.134
257.0	0.127
280.0	0.108
304.0	0.092
317.54	0.088
325.03	0.088
332.50	0.088

TABLE 2

Data Curve A Fig. 3

Numerical Internal Friction Data for 99.999%

Al Wire Diameter 0.0005m

Annealed at 250°C for 5 Hours

Temperature °C	Internal Friction (Q^{-1})
70.12	0.006
102.00	0.013
122.31	0.019
137.50	0.033
158.78	0.057
194.80	0.105
222.48	0.119
240.00	0.119
267.18	0.104
300.00	0.070
320.00	0.054
333.58	0.047

TABLE 3

Data Curve B Fig. 3

Numerical Internal Friction Data for 99.999%

Al Wire Diameter 0.0005m

Annealed at 250°C for 6 Hours

Temperature °C	Internal Friction (Q^{-1})
61.89	0.003
96.75	0.008
116.50	0.012
135.00	0.020
154.13	0.035
176.81	0.059
194.90	0.079
227.50	0.104
246.20	0.103
260.00	0.088
276.59	0.075
290.00	0.062
307.12	0.054
312.50	0.047
335.00	0.038

TABLE 4

Data Curve C Fig. 3

Numerical Internal Friction Data for 99.999%

Al Wire Diameter 0.0005m

Annealed at 250°C for 7 Hours

Temperature (°C)	Internal Friction (Q^{-1})
60.00	0.005
97.05	0.008
145.00	0.020
169.11	0.030
137.52	0.048
206.19	0.065
218.14	0.078
239.82	0.089
265.00	0.079
280.00	0.059
291.56	0.049
307.63	0.042
325.00	0.034
334.87	0.032

TABLE 5

Data Curve D Fig. 3

Numerical Internal Friction Data for 99.999%

Al Wire Diameter 0.0005m

Annealed at 250°C for 10 Hours

Temperature (°C)	Internal Friction (Q^{-1})
58.95 C	0.002
72.55	0.004
101.05	0.005
132.48	0.012
164.59	0.023
202.35	0.044
212.50	0.051
228.05	0.055
238.82	0.055
252.00	0.050
261.15	0.043
278.27	0.035
296.88	0.030
315.98	0.028
334.15	0.026
344.87	0.026

TABLE 6

Data Curve E Fig. 3

Numerical Internal Friction Data for 99.99%

Aluminium Wire Diameter 0.00025m

Annealed at 200°C for 4 Hours

Temperature	Internal Friction
35.03	0.004
62.51	0.004
94.86	0.006
117.52	0.013
183.25	0.060
195.08	0.092
227.84	0.120
261.01	0.114
285.00	0.086
317.55	0.072
340.14	0.064
371.02	0.059

TABLE 6

Data Curve A Fig. 4

Numerical Internal Friction Data for 99.99%

Aluminium Wire Diameter 0.00025m

Annealed at 300°C for 4 Hours

Temperature °C	Internal Friction (Q^{-1})
50.15	0.006
75.21	0.006
115.00	0.006
160.56	0.011
194.50	0.023
205.03	0.036
212.33	0.052
220.00	0.073
230.11	0.102
240.61	0.110
253.72	0.109
275.92	0.096
295.01	0.080
325.32	0.062
350.73	0.056

TABLE 7

Data Curve B Fig. 4

Internal Friction Data for 99.99%

Al Wire Diameter 0.00025m

Annealed at 400°C for 4 Hours

Temperature °C	Internal Friction (Q^{-1})
130.37	0.006
160.76	0.009
176.21	0.013
198.70	0.023
222.50	0.37
233.06	0.054
240.00	0.071
242.96	0.083
253.63	0.092
274.83	0.089
283.14	0.081
305.21	0.067
330.42	0.054
362.55	0.048

TABLE 8

Data Curve C Fig. 4

Numerical Internal Friction Data for 99.99%

Al Wire Diameter 0.00025m

Annealed at 500°C for 4 Hours

Temperature °C	Internal Friction (Q^{-1})
135.26	0.006
150.46	0.006
169.94	0.010
210.00	0.020
226.31	0.028
239.88	0.044
257.38	0.060
268.42	0.076
288.26	0.078
315.01	0.056
342.52	0.047

TABLE 9

Data Curve D Fig. 4

Numerical Internal Friction Data for 99.99%

Al Wire Diameter 0.00025m

Annealed at 600°C for 4 Hours

Temperature °C	Internal Friction
175.42	0.010
197.38	0.013
220.18	0.018
247.55	0.034
255.04	0.046
271.12	0.056
293.49	0.050
312.62	0.043
325.72	0.041

TABLE 10

Data Curve E Fig. 4

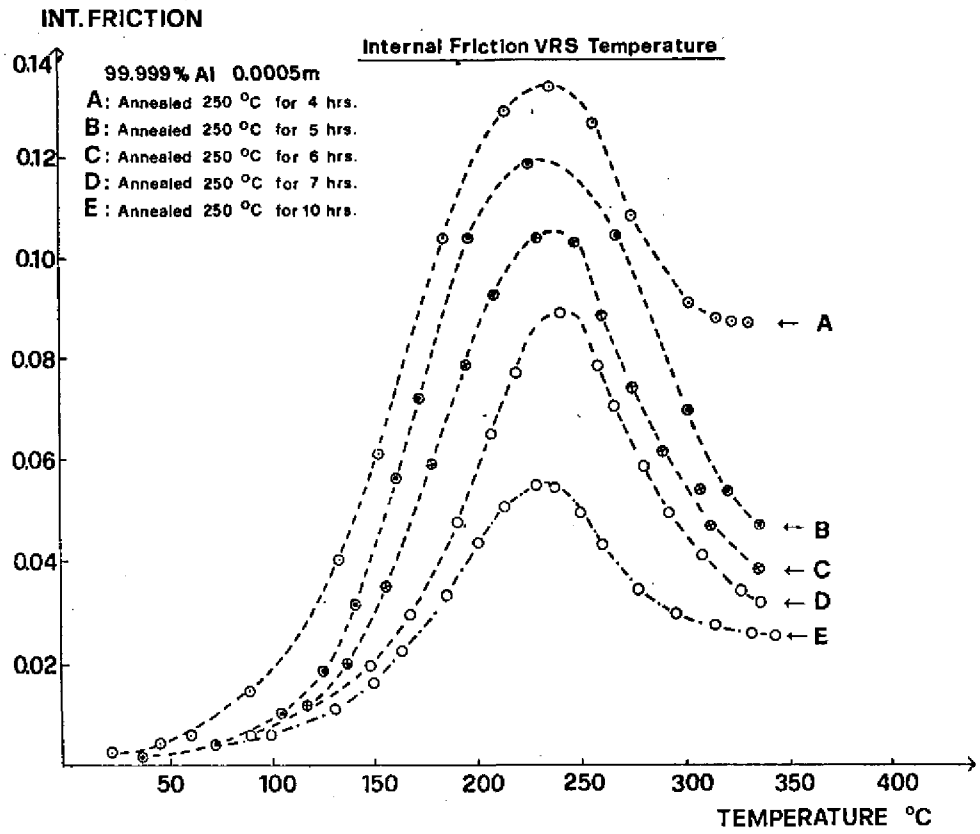

Fig. 3

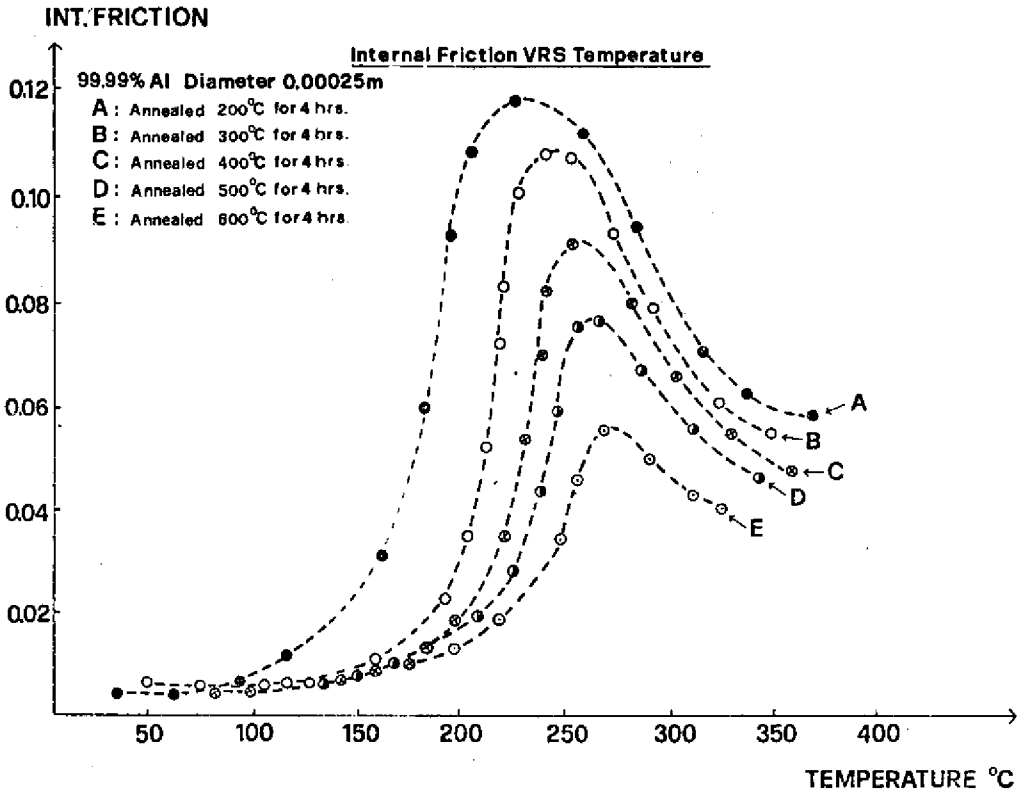
INT. FRICTION
Internal Friction VRS Temperature
99.99% Al Diameter 0.00025m
A : Annealed 200°C for 4 hrs.
B : Annealed 300°C for 4 hrs.
C : Annealed 400°C for 4 hrs.
D : Annealed 500°C for 4 hrs.
E : Annealed 600°C for 4 hrs.
0.12
0.10
0.08
0.06
0.04
0.02
50
100
150
200
250
300
350
400
TEMPERATURE °C
A
B
C
D
E

Fig. 4

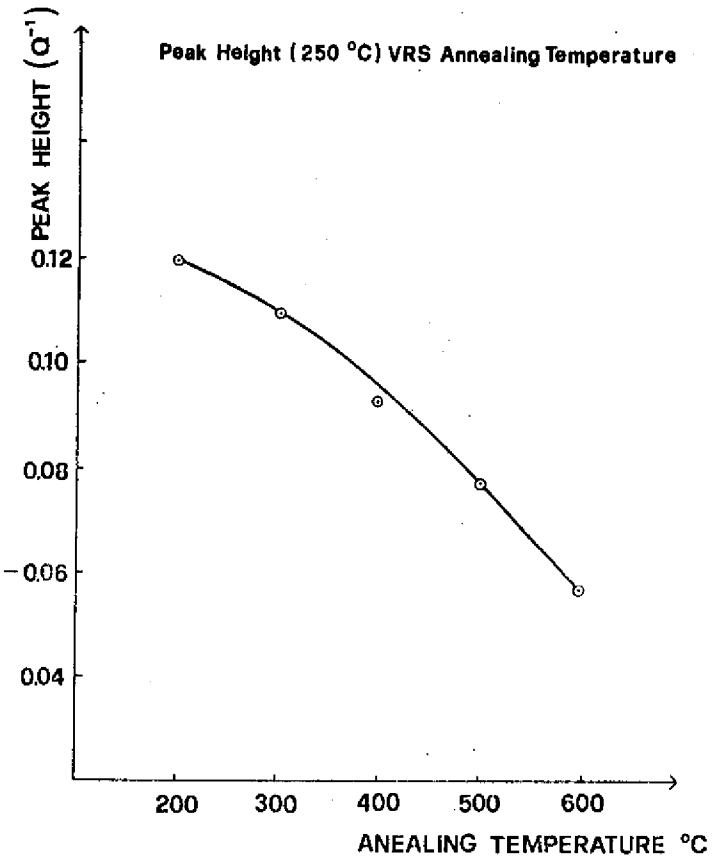
Peak Height (250 °C) VRS Annealing Temperature
PEAK HEIGHT (Q^{-1})
0.12
0.10
0.08
−0.06
0.04
200
300
400
500
600
ANEALING TEMPERATURE °C

Fig.5

CURRENT ICTP PUBLICATIONS AND INTERNAL REPORTS

IC/82/1 INT.REP.* TH.M. EL-SHERBINI - Excitation mechanisms in singly ionized krypton laser.

IC/82/2 INT.REP.* CHR.V. CHRISTOV, I.I. DELCHEV and I.Z. PETKOV - On direct mechanism of light-particle emission in incomplete-fusion reactions

IC/82/3 F. CLARO and V. KUMAR - Phase diagrams for a square lattice with two- and three-body interactions.

IC/82/4 E. ROMAN, G. SENATORE and M.P. TOSI - A simple model for the surface energy of ionic crystals.

IC/82/5 INT.REP.* G.A. CHRISTOS - "Loop the loop".

IC/82/6 H.R. KARADAYI - L-R asymmetry in GUT's.

IC/82/7 INT.REP.* YASUSHI FUJIMOTO and JAE HYUNG YEE - The electron magnetic moment at high temperature.

IC/82/8 INT.REP.* T.S. SANTHANAM - Charge structure of quarks and the number of valence quarks in the nucleon.

IC/82/9 INT.REP.* TH.M. EL-SHERBINI and A.A. RAHMAN - Auto-ionizing states in MgI.

IC/82/10 INT.REP.* K.P. JAIN and G.S. JAYANTHI - Quasibound exciton-LO phonon intermediate state in multi-phonon Raman scattering of semiconductors.

IC/82/11 T. SRIVASTAVA - A two-component wave equation for particles of spin $\frac{1}{2}$ and non-zero rest mass (Part II).

IC/82/12 INT.REP.* T.S. SANTHANAM and S. MADIVANANE - The structure of the Hamiltonian in a finite-dimensional formalism based on Weyl's quantum mechanics.

IC/82/13 J.A. MAGPANTAY, C. MUKKU and W.A. SAYED - Hot gauge theories in external electromagnetic fields.

IC/82/14 H.R. KARADAYI - The derivation of the conventional basis for the simple Lie algebra generators.

IC/82/15 H.R. KARADAYI - SO(14) unification of 3+1 families.

IC/82/16 W. NAHM - The construction of all self-dual multimonopoles by the ADHM method.

IC/82/17 B. GRUBER and T.S. SANTHANAM - Indecomposable representations for parabose algebra.

IC/82/18 R. PERCACCI and S. RANDJBAR-DAEMI - Kaluza-Klein theories on bundles with homogeneous fibres - I.

IC/82/19 W. ANDREONI, M. ROVERE and M.P. TOSI - Co-ordination of heterovalent cation impurities in molten salts.

IC/82/20 INT.REP.* L. SMRČKA - A "quadratized" augmented plane wave method.

IC/82/21 V. de ALFARO, S. FUBINI and G. FURLAN - Some remarks about quantum gravity.

IC/82/22 G. GHABRIER, G. SENATORE and M.P. Tosi - Ionic structure of solutions of alakali metals and molten salts.

THESE PREPRINTS ARE AVAILABLE FROM THE PUBLICATIONS OFFICE, ICTP, PO BOX 586, I-34100 TRIESTE, ITALY.

IC/82/23 INT.REP.* SUN KUN OH - Mass splitting between B^+ and B^0 mesons.

IC/82/24 INT.REP.* A. BREZINI - Self-consistent study of localization near band edges.

IC/82/25 INT.REP.* C. PANAGIOTAKOPOULOS - Dirac monopoles and non-Abelian gauge theories.

IC/82/26 CAO CHANG-qi and DING XING-fu - Intermediate symmetry $SU(4)_{EC} \times SU(2)_L \times U(1)_Y$ and the SU(N) unification series.

IC/82/27 H.B. GHASSIB and S. CHATTERJEE - ^{4}He-impurity effects on normal liquid ^{3}He at low temperatures - I: Preliminary ideas and calculations.

IC/82/28 C. PANAGIOTAKOPOULOS, ABDUS SALAM and J. STRATHDEE - Supersymmetric local field theory of monopoles.

IC/82/29 INT.REP.* G.A. CHRISTOS - Concerning the proofs of spontaneous chiral symmetry breaking in QCD from the effective Lagrangian point of view.

IC/82/30 INT.REP.* M.I. YOUSEF - Diffraction model analyses of polarized ^{6}Li elastic scattering.

IC/82/31 L. MIZRACHI - Electric-magnetic duality in non-Abelian gauge theories.

IC/82/32 INT.REP.* W. MECKLENBURG - Hierarchial spontaneous compactification.

IC/82/33 C. PANAGIOTAKOPOULOS - Infinity subtraction in a quantum field theory of charges and monopoles.

IC/82/34 INT.REP.* M.W. KALINOWSKI, M. SEWERYNSKI and L. SZYMANOWSKI - On the F equation.

IC/82/35 INT.REP.* H.C. LEE, LI BING-AN, SHEN QI-XING, ZHANG MEI-MAN and YU HONG - Electroweak interference effects in the high energy $e^+ + e^- \rightarrow e^+ + e^-$ + hadrons process.

IC/82/36 G.A. CHRISTOS - Some aspects of the U(1) problem and the pseudoscalar mass spectrum.

IC/82/37 C. MUKKU - Gauge theories in hot environments: Fermion contributions to one-loop.

IC/82/38 INT.REP.* W. KOTARSKI and A. KOWALEWSKI - Optimal control of distributed parameter system with incomplete information about the initial condition.

IC/82/39 INT.REP.* M.I. YOUSEF - Diffraction model analysis of polarized triton and ^{3}He elastic scattering.

IC/82/40 INT.REP.* S. SELZER and N. MAJLIS - Effects of surface exchange anisotropy in Heisenberg ferromagnetic insulators.

IC/82/41 INT.REP.* H.R. HAROON - Subcritical assemblies, use and their feasibility assessment.

IC/82/42 W. ANDREONI and M.P. TOSI - Why is AgBr not a superionic conductor?

IC/82/43 N.S. CRAIGIE and J. STERN - What can we learn from sum rules for vertex functions in QCD.

IC/82/44 INT.REP.* ERNEST C. NJAU - Distortions in power spectra of digitised signals - I: General formulations.